Optimization of physical properties of Ag - Li nanoferrites via the facile citrate precursor method

Nagwa A.Okasha[1], Maha M.Alsyed[2]*

1.Physics Department, GirlsCollege, AinShamsUniversity, Cairo, Egypt.

2. Materials Science Lab (1), Physics Department, Faculty of Science, CairoUniversity, Giza, Egypt.

Abstract

Silver-substituted lithium ferrites ($Li_{0.5-x}Ag_xFe_{2.5}O_4$; x=0, 0.025, 0.05, 0.075, 0.1nanoparticles were prepared via citrate autocombustion method. All the ferritesamples have been characterized using XRD, TEM, χ_M, VSM, and ac electricalconductivity. The crystallite size is between 44 to 49 nm. The saturation magnetizationreaches a maximum value of 69 emu/g. mole higher than the undoped sample at 50emu/g. mole. The Curie temperature improves 1.1 times on the undoped sample. Theincrease in the dielectric constant by Ag^+ depends on the electronic configuration of thedifferent Ag content .

Keywords:Ag- nanoferrites; Citrate precursor method; Magnetic properties; Dielectric properties.

1. Introduction

Ferrites have a vast range of applications from microwave to radio frequencies, and have a very low conductivity, which is an important requirement for microwave applications. In the spinel structure magnetic ions are distributed between two different lattice sites, tetrahedral (A) and octahedral (B) sites. Magnetic as well as electrical properties of these ferrites depend on the distribution of cations at the different sites as well as preparation conditions **(Shipway,A. N. 2000), (Hao,E. 1999), (Gilbert, I.P. 2002), (Dobrazanski,L.A. 2004),** pharmaceuticals **(Dobrzanski,L.A. 2006) , paints (Chicinas,I. 2005),** coatings**(Kumar,K.V. 2001), (Horvath, M.P. 2000),** superconductors **(Tsay,C.Y. 2000),** semiconductors **(Correa , M. A. 1998), (Lemon,B. I. 2000), (Shokrollahi,H. 2006),** and catalysis**(Shokrollahi,H. 2007), (Yamamoto S. 2001).**

Corresponding author:M. Mohsen; mahamohsen245@yahoo.com

In recent years, nanotechnology has been the subject of many researchers all over the world because of novel phenomena and special properties exhibited by nanoparticles. The properties of any material in the bulk state are known to vary drastically and unimaginably as the bulk material approaches the nanoscale**(Guozhong, Cao 2003), (Buscaglia, M.T. 2004).**

The unusual properties are attributed to size, shape and distribution of particles in the material, which in turn depend on the method of synthesis. Substitution of non-magnetic ions at either site alters the A–A or B–B and A–B interaction, which leads to a significant change in their physical properties.

Pure and substituted lithium ferrites form an important class of magnetic material due to their high saturation magnetization, resistivety and Curie temperature. Magnetic and electrical properties of ferrites have been found to be sensitive to their composition and processing techniques **(Kharabe, R.G. 2006), (Ahmed, M.A. 2008)**and used in cathode materials in lithium ion **batteries (Wolska, E. 1997), (Obrovac, M.N. 1998).** Also they are used in microwave applications due to their high resistivety and low eddy current losses **(Dahn, J.R. 1990), (Argentina, G.M. 1974).**

Among the chemical synthesis methods, citrate precursor method appear to be simple and convenient, which gives more uniformity of particles and magnetic properties are immensely improved **(Manoharan, S.J. 1992), (Soibam, I. 2009).**

The role of substituent in modifying the properties of basic ferrites has been widely studied. Development of high quality, low cost and low loss for high frequency ferrite material for power applications is an ever challenging aspect for researchers. Substituted lithium ferrites may be useful material for such applications because of their modified magnetic and electrical properties (**Jiang,J. 2007), (Yen-Pei 2005), (Verma, V. 2009).**

Many authors have studied some physical properties such as frequency dependence of the dielectric constant, dielectric loss tangent and ac conductivity of Li–Ni **(Reddy V.P. 1994),** Li–Co**(Venudhar, Y.C. 2002),** Li–Mg **(Bellad, S.S. 2000),** and Li–Ge**(Ravinder,D. 2003)** ferrite systems. However, no reports have been found in the literature on physical properties of Ag-substituted lithium ferrites while,

Very few studies are available on silver ferrites **(Kluthe,C. 2003), (Dogra, A. 2004), (Hong, S.H. 2005), and (Okasha N. 2008).** Almost all silver compounds with predominantly ionic bonding properties are light sensitive and in many cases also thermally sensitive. Though there have been a few investigations on silver such as Ag–Mn**(Sperka,G. 1988)** and Ag–Bi **(Song,KH. 1991)**, its various properties such as thermal decomposition kinetics, structure, magnetic measurements **(Scatturin, V. 1960),** and resonance Raman work were studied by **(Chang, FM. 1984).**

Therefore, in the present work, we are going to deal with the synthesis of silver nanoparticles substitution lithium ferrites; $Li_{0.5-x}Ag_xFe_{2.5}O_4$; x=0, 0.025, 0.05, 0.075, 0.1 via citrate autocombustion method to investigate their physical properties and deduce the optimum silver concentration.

2. Material and Methods

2.1. Samples preparation

Ultrafine particles of $Li_{0.5-x}Ag_xFe_{2.5}O_4$; x=0, 0.025, 0.05, 0.075, 0.1 nanoferrites were prepared by the citrate precursor method at room temperature **(Ahmed M.A. 2010).** The raw materials used were analytical reagent grade lithium nitrate $LiNO_3$, silver nitrate [$AgNO_3$], iron nitrate [Fe $(NO_3)_3$ $9H_2O$], and citric acid[$C_6H_8O_7$. H_2O]. Stoichiometric amounts of the metal nitrates were dissolved in a minimum amount of doubly distilled water to get a clear solution form the citrate-precursor mixture. A drop wise of ammonia solution was added to the precursor solution to adjust the pH value to about 7. The mixed metal nitrate solution was then added to the citric acid solution in 1:1 molar ratio. The resulting solution was continuously heated to allow evaporation and to obtain a dried product in the form of uniformly colored gray fibers containing all the cations homogeneously mixed together.

2.2. characterization

X-ray characterization of the as-prepared powder samples was carried out using an X-ray diffractometeron a Proker D_8 advance X-ray diffractometer using CuKαradiation (λ=1.54056˚A) in the range of 20- 80°. The crystalline phases were identified using the International Centre for Diffraction Data (ICDD) card number 17- 0115(D). Transmission electron microscope (TEM, JEOL – 1010) used to observe the

morphology and particle size of the samples. Infrared spectra (FTIR) of the investigated samples were recorded using JASCO FT/Ie6100 spectrometer in the range 400- 4000 cm^{-1} in the KBr medium. Measurements of dc magnetic susceptibility χ_M were carried out using Faraday's method at different temperatures as a function of magnetic field intensities; 883, 1172, and 1452 Oe. The accuracy of measuring temperature in the magnetic susceptibility measurements was $\pm 1^oC$. Room temperature magnetization measurements and hysteresis loops was carried out up to the maximum field of 8kOeat room temperatureusing a vibrational sample magnetometer (VSM; 9600-1, LDJ, USA).The RLC Bridge (Hioki model 3531 Japan) was used to measure the *ac* electrical resistivety as well as the dielectric constant (ε') and dielectric loss factor (ε") of the investigated samples that were carried out at different temperatures from room temperature up to 800K at various frequencies from 400 kHz to 4MHz. The thermoelectric power (α) was calculated using the relation: $\alpha = \Delta V/\Delta T$; where ΔV is the voltage measured across the sample, ΔT the temperature difference between the two surfaces of the sample which is fixed at =10°C.

3. Results and Discussion

The formation of $Li_{0.5-x}Ag_xFe_{2.5}O_4$; x=0, 0.025, 0.05, 0.075, 0.1 was confirmed from the characteristic powder XRD pattern shown in Fig. (1).Analysis of the diffraction pattern of all samples reveals the formation of single phase cubic spinel structure as indexed and compared with ICDD Card no. 17- 0115(D). The data shows considerable line broadening, indicating that the particles are nanosized with average crystallite sizes (t) and lattice constant (a) that isshown at Fig. (2) Andlisted in Table (1).

It is revealing that, the value of (a) increases with increasing (x) up to 0.075 then decreases. The observed linear decrease in (a) with (x) is due to the smaller ionic radius of Li^+ (0.67A°) ions and the larger ionic radius of Ag^+ (1.26 A°) which reside on the grain boundary causes shrinkage in the lattice as well as decrease in the lattice constant and crystallite size. The average crystallite size (t) was calculated from X-ray line broadening using (311) peaks and Debye–Sherrer's equation **(Cullity B.D. 2001)** and the data are reported in Table (1). It is clear that, as Ag concentration

increases, lattice constant increases. The increases of lattice constant could be explained on the basis of ionic radii, where the radius of Li^+ (0.67A˚) is smaller than that of Ag^+ (1.26 Å). Besides, the crystallite size increases with increasing Ag content up to x = 0.075 then decreases. This could be explained on the basis of the statistical cation redistribution among the tetrahedral and octahedral sites.

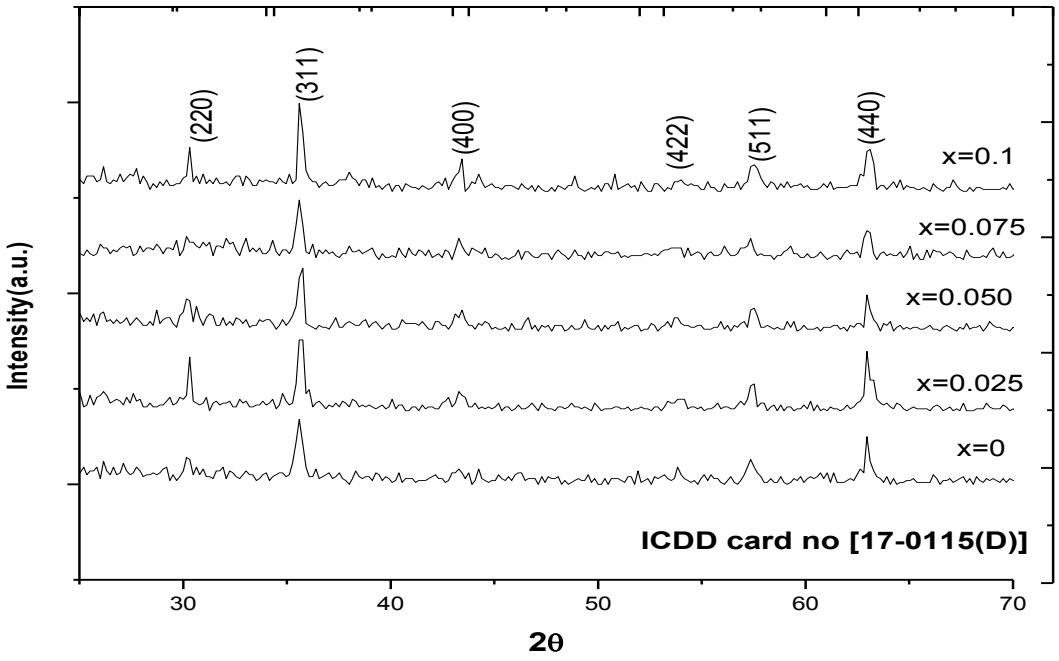

Fig. (1): XRD patterns for $Li_{0.5-x}Ag_xFe_{2.5}O_4$; $0 \leq x \leq 0.1$ nanoferrites.

Table (1): XRD parameters of $Li_{0.5-x}Ag_xFe_{2.5}O_4$ nanoferrite; $0 \leq 0.1$.

(x)	a(A)	$t_{(XRD)}$	$t_{(TEM)}$
0.000	8.3422	44	41
0.025	8.3429	47	39
0.050	8.3433	49	38
0.075	8.3376	56	37
0.100	8.3382	51	47

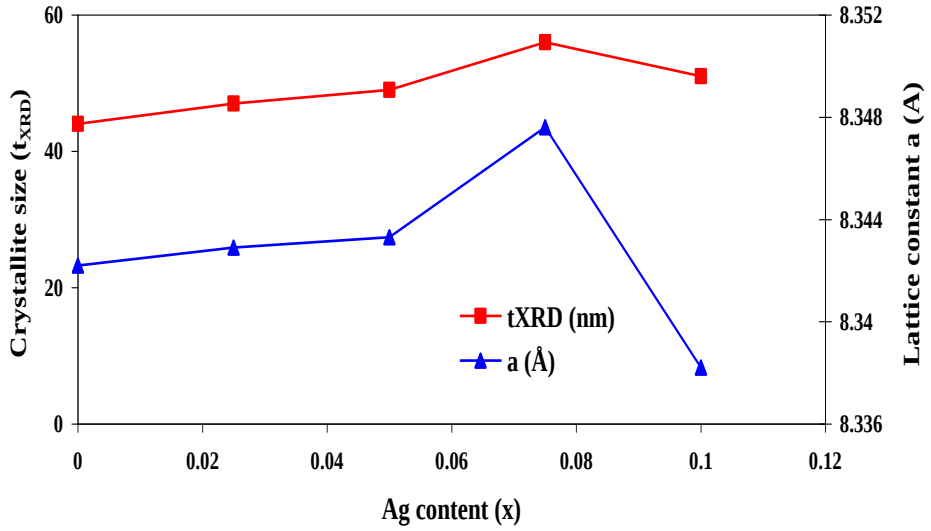

Fig. (2): The dependence of the lattice constant (a) and the crystallite size (t_{XRD}) on the Ag content (x) on for $Li_{0.5-x}Ag_xFe_{2.5}O_4$nanoferrites system.

Figure (3) shows the typical TEM images of $Li_{0.5-x}Ag_xFe_{2.5}O_4$nanoferrites (with average crystallite size of about 48 nm as determined from XRD). The maximum value lies between 37 and 46 nm, in good agreement with XRD crystallite size. Besides, most of the particles appear spherical in shape however some elongated particles are also present as shown in the TEM images. Some moderately agglomerated particles as well as separated particles are present in the images. Besides, the diffraction rings (inset) are those of a typical spinel structure. The diffraction rings correspond to the reflection off (220), (311) (400), and (440) planes.

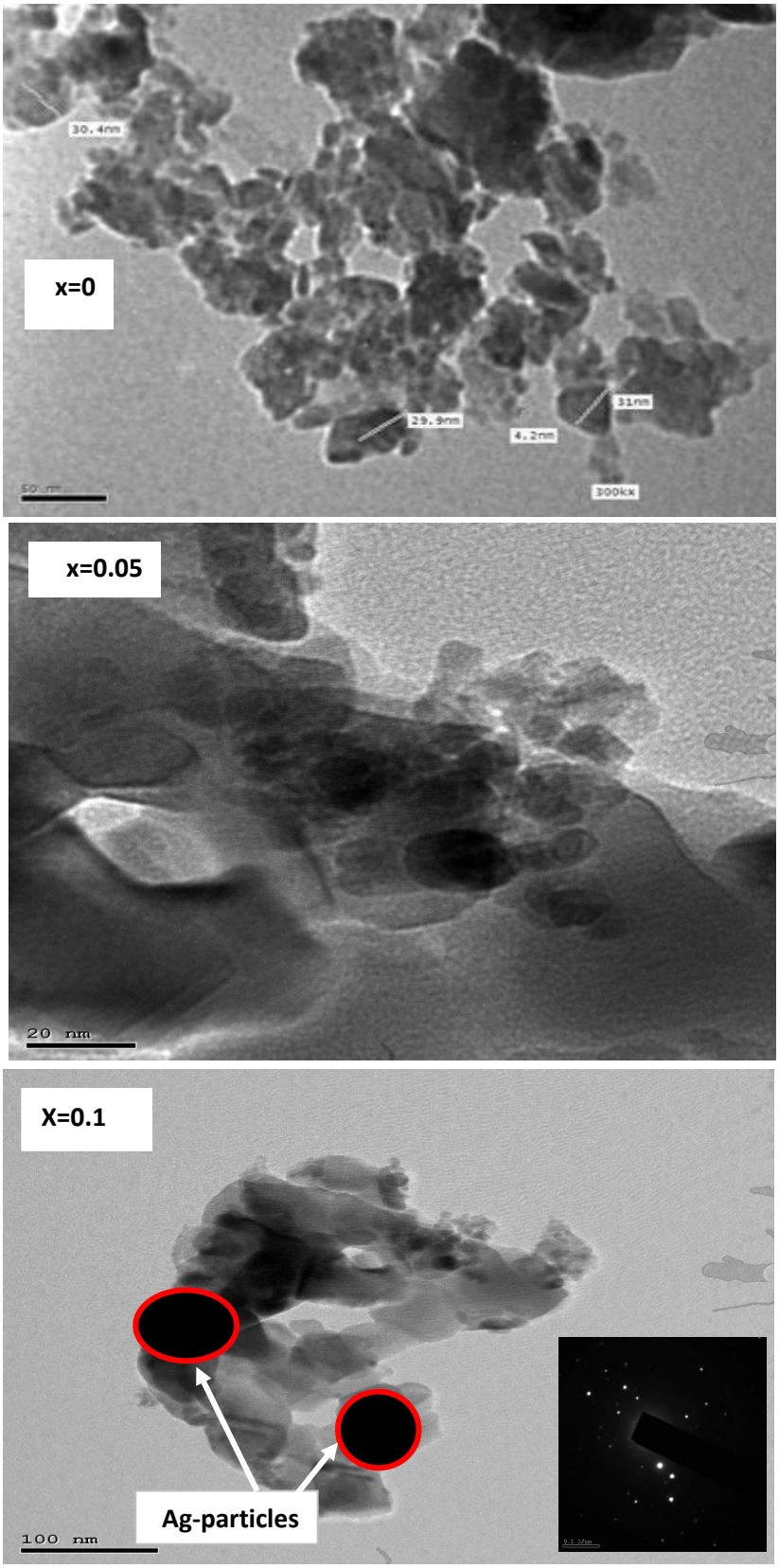

Fig. (3): Typical TEM micrograph of $Li_{0.5-x}Ag_xFe_{2.5}O_4$ nanoferrites.

The field dependence of molar magnetic susceptibility χ_M at different temperature and magnetic intensity for the investigated samples was carried out in order to define the dynamic behavior of the particle are shown in .Fig. (4: a–e).The results reveal the normal behavior of the magnetic susceptibility (χ_M) of the ferrite materials in which (χ_M) is slightly decreased with increasing temperature and decreases suddenly at the Curie temperature (T_C). This behavior can be explained according to; at low temperature (ferrimagnetic), the thermal energy which affects on the sample is not enough to overcome the impact of the magnetic field which aligns the spins in its direction. The result is the slow decrease of (χ_M) with increasing temperature. While, at high temperature region (paramagnetic), the thermal energy increases the lattice vibration as well as the disordered state of spins causing the rapid decrease in (χ_M).

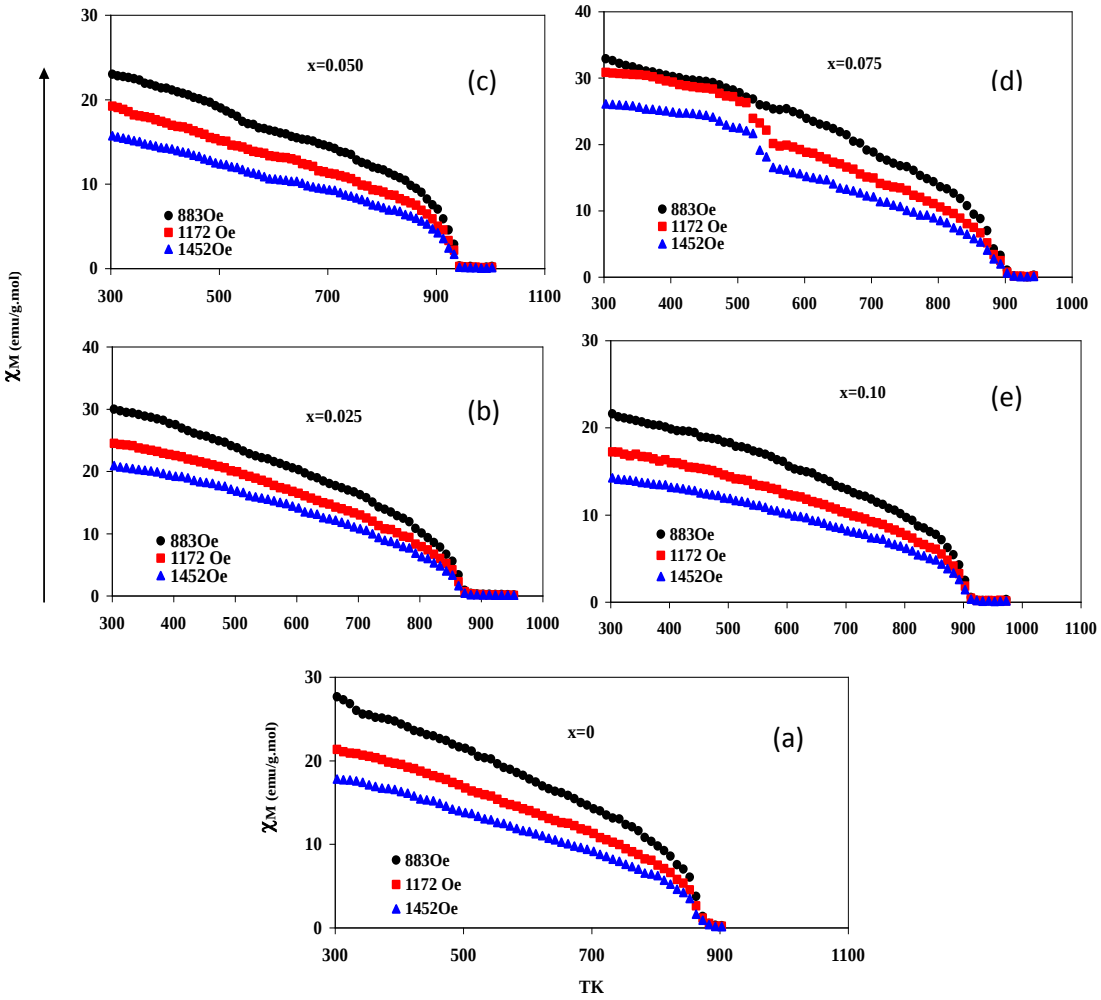

Fig. (4: a- e): Variation of χ_M at different temperature (TK) as a function of magnetic field intensity (H) for $Li_{0.5-x}Ag_xFe_{2.5}O_4$nanoferrites system

The variation of Curie temperature T_C with Ag content (x) was observed in Fig. (5a). Introducing Ag^+ ions with large ionic radius (1.26A°) increases the ratio of Fe^{2+}/Fe^{3+} on the B sites, after that, some of Fe^{2+} ions could migrate from B to A sites which decreases directly the net magnetization of the system. Variation in the oxygen content due to the difference between the valances of Fe^{3+} and Ag^+ consider another reason can affect the interaction distance and angle lead to a change in the magnetic interaction "DH. Han 1994". In other words, the exchange interactions between the magnetic ions on A and B sublattices increase with both the density and the magnetic moment of the magnetic ions. Greater amount of thermal energy is required to offset the effects of exchange interactions. The increase of Ag content after x = 0.075, decreases the number of iron (Fe^{3+}) ions available on B sites. Consequently, a redistribution of the metal cations takes place in the spinel matrix resulting in an increase in T_C. Figure (5b) shows the effective magnetic moment μ_{eff} at different Ag content (x) as a function of magnetic field intensity. The replacement of Li^{2+} from A to B sites on the expense of Fe^{3+} which migrate to A sites as Fe^{2+} has larger ionic radius causes disruption of the magnetic ordering of Li^{2+} and Fe^{3+} ions leading to decrease of μ_{eff}as mentioned before.Besides, In Li-ferrite which is inverted spinel, the magnetic moment of the tetrahedral ions is 5BM and that of octahedral ions is 3+5BM which is the sum of the magnetic moment of Li^+ and $Fe^{3+.}$ When comparing the exchange interaction constant of A and B sites one can find that, the AB interaction is by far the greatest one. The weakest exchange interaction will be the AA one. The value of the exchange energy is expected to be affected by the deviations in the oxygen parameter. In most ferrites, where the oxygen ions are displaced in such a way that, in the AB interaction the distance between the A and the O^{-2} ions is increased and that between the B and O^{2-} ions is decreased. Accordingly the AA interaction is reduced and the BB interaction is increased which gives the largest value of AB interaction. In the third region after (x = 0.075), Ag^+ ions increased on the A sites to the limit at which the concentration does not affect the magnetic susceptibility value. This is because Li-ferrite is predominant, representing skeleton of the sample. The presence of silver ions in the investigated ferrite improves the Curie temperature 1.1 times on the undoped sample.

Table (2): Dependence of Ag content on; Curie temperature (T_C), the effective magnetic moment (μ_{eff}), and the molar magnetic susceptibility (χ_M) at room temperature (RT) for $Li_{0.5-x}Ag_xFe_{2.5}O_4$nanoferrites.

Formula	Ag content(x)	T_C (K)	μ_{eff} (BM) 883 Oe	μ_{eff} (BM) 1172 Oe	μ_{eff} (BM) 1452 Oe	χ_M (emu/g.mole)
$Li_{0.5}Fe_{2.5}O_4$	0	867	7.0	6.6	6.3	21.3
$Li_{0.475}Ag_{0.025}Fe_{2.5}O_4$	0.025	893	6.4	6.0	5.5	22.5
$Li_{0.45}Ag_{0.05}Fe_{2.5}O_4$	0.05	900	7.4	6.8	6.4	19.2
$Li_{0.425}Ag_{0.075}Fe_{2.5}O_4$	0.075	915	7.8	7.3	6.7	24.9
$Li_{0.4}Ag_{0.1}Fe_{2.5}O_4$	0.1	896	6.7	5.8	5.4	17.2

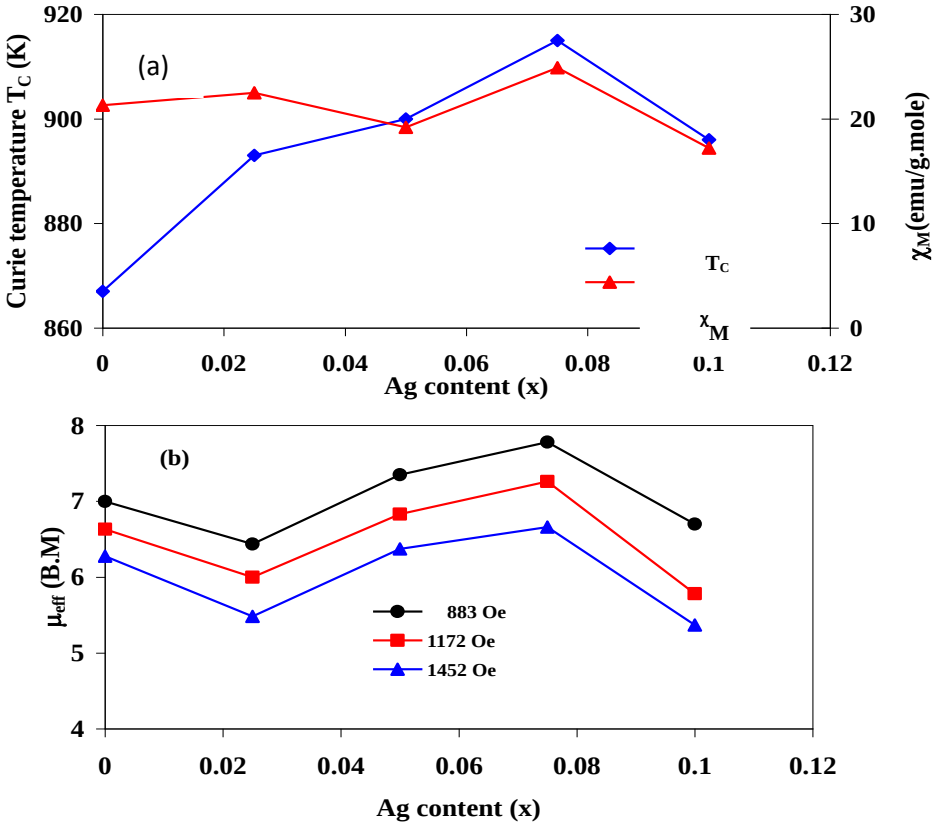

Fig. (5: a, b): a. Dependence of the Curie temperature (T_C) and the molar magnetic susceptibility (χ_M) on the Ag content (x). b. The dependence of the effective magnetic moment μ_{eff} on the Ag content for $Li_{0.5-x}Ag_xFe_{2.5}O_4$; $0.0 \leq x \leq 0.1$nanoferrites.

Figure (6) shows the room temperature hysteresis loop of the powder samples for various silver substitutions. It is clear that the samples have soft ferrimagnetic behavior for all concentrations. This reveals that the samples are in nanosized forms, as pointed out in the XRD patterns. The values of saturation magnetization (M_s), remanence magnetization (M_r) and coercive field (H_c) are listed in Table (3). It can be seen that, the variation pattern of specific saturation magnetization (M_s) as a function of Ag content shows an increase and reaches a maximum value of 69 Oe at x = 0.075. The changes in magnetic property of M_s, is due to the influence of the cationic stoichiometry and their occupancy in the specific sites where formation of dead layer on the surface, existence of random canting of particle surface spins "GM. Kale 1993".Moreover, the magneton number (η_B) (the saturation magnetization per formula unit in Bohr magneton) at 300 K obtained from magnetization data for all the samples are summarized in Table (3). The magnetic moment per formula unit in Bohr magneton (η_B) was calculated by using the relation:

$$\eta_B = MW * M_s / 5585$$

Where,
MW = Molecular weight of composition (in grams)
M_s =Saturation magnetization (in Oe)
5585 = Magnetic factor

In calculating magnetic moment (η_B), we have considered A–B interaction and cation distribution obtained from X-ray intensity ratio calculations. In the present study, Ag^+ ions occupy tetrahedral A-site and Li^+ ions are distributed over the tetrahedral A and octahedral B sites. Due to nonmagnetic substitution of Ag^+ ions at A-site, tetrahedral (A) sub-lattice magnetic moment will decrease. However, magnetic moment of A-site is less than that of magnetic moment of B-site for all the compositions. Thus, the net magnetic moment (η_B) increases with the increase Ag content x up to x=0.075 then decrease as mentioned before.

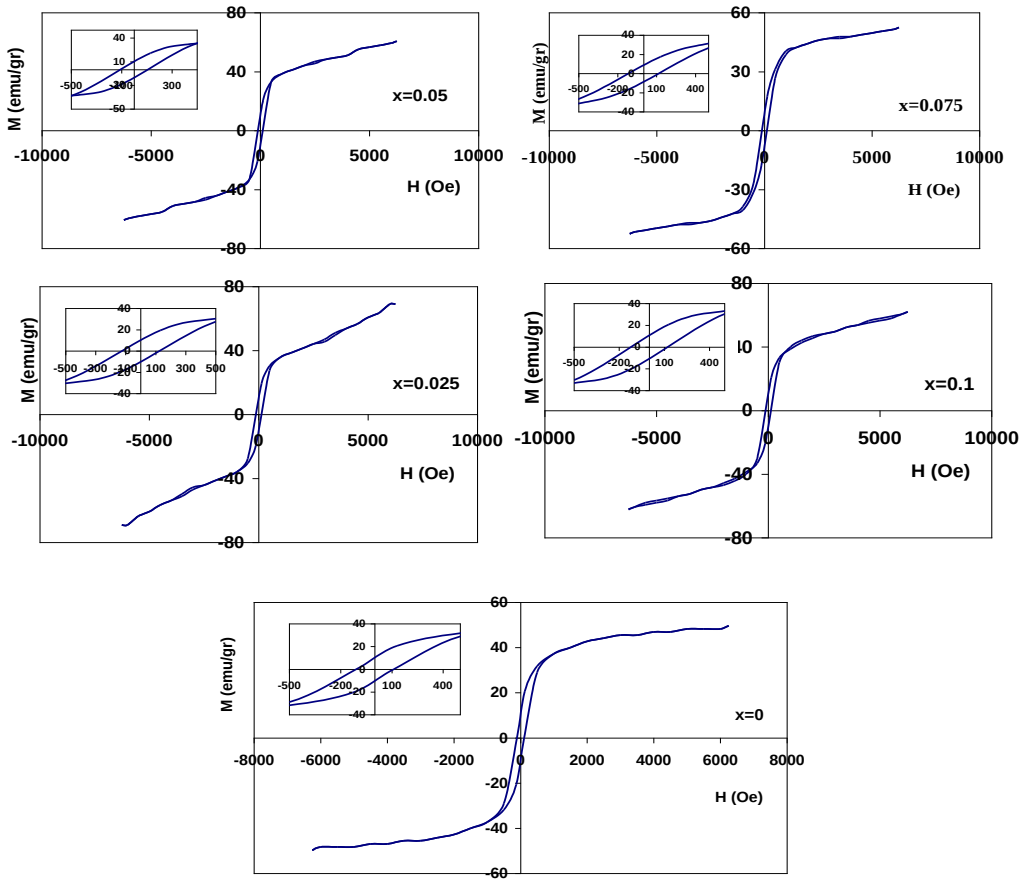

Fig.(6): The hysteresis loop behavior for $Li_{0.5-x}Ag_xFe_{2.5}O_4$; $0 \leq x \leq 0.1$ nanoferrite system.

Table (3): Variation of the saturation magnetization (M_s), remanence magnetization (M_r), coercivity (H_c), squareness ratio (M_r/M_s), and magnetic moment (η_B) for $Li_{0.5-x}Ag_xFe_{2.5}O_4$nanoferrites.

Formula	Ag content(x)	M_s(emu/g)	M_r(emu/g)	H_C(Oe)	M_r/M_s	η_B (B.M)
$Li_{0.5}Fe_{2.5}O_4$	0	50	11	110	0.22	1.84
$Li_{0.475}Ag_{0.025}Fe_{2.5}O_4$	0.025	62	10	118	0.16	2.42
$Li_{0.45}Ag_{0.05}Fe_{2.5}O_4$	0.05	61	9	108	0.15	2.31
$Li_{0.425}Ag_{0.075}Fe_{2.5}O_4$	0.075	69	16	120	0.23	2.59
$Li_{0.4}Ag_{0.1}Fe_{2.5}O_4$	0.1	52	7	116	0.13	2.02

Figure (7) represents the variation of ε' as a function of the absolute temperature at the applied frequencies 40 kHz – 4MHz for the samples $Li_{0.5-x}Ag_xFe_{2.5}O_4$; $0.0 \leq x \leq 0.1$ nanoferrites. It is clearly shows for all frequencies ε' increases with increasing temperature. In the first region ε' is increased slowly with temperature up nearly to T = 500 K for all the samples, this means that the thermal energy given to the system is not sufficient enough to free the localized dipoles and to orient them in the field direction. In the second region of temperature, the thermal energy liberates more localized dipoles, and the field tries to align them in its direction, leading to an increase of the polarization as well as of ε'. The increase in ε' up to the transition temperature then decreases for all doped samples is due to the various contributions of the polarization, especially the interfacial one, which acts in the insulating region separating the conducting grains "J.R. Hook 1991". Besides, the decrease in ε' with increasing frequency is due to the fast alternation of the field, where the alternation of the dipoles as well as the friction between them leads to an increase in the quantity of heat dissipated, so the aligned dipoles will be disturbed with the result of a decreasing ε'.

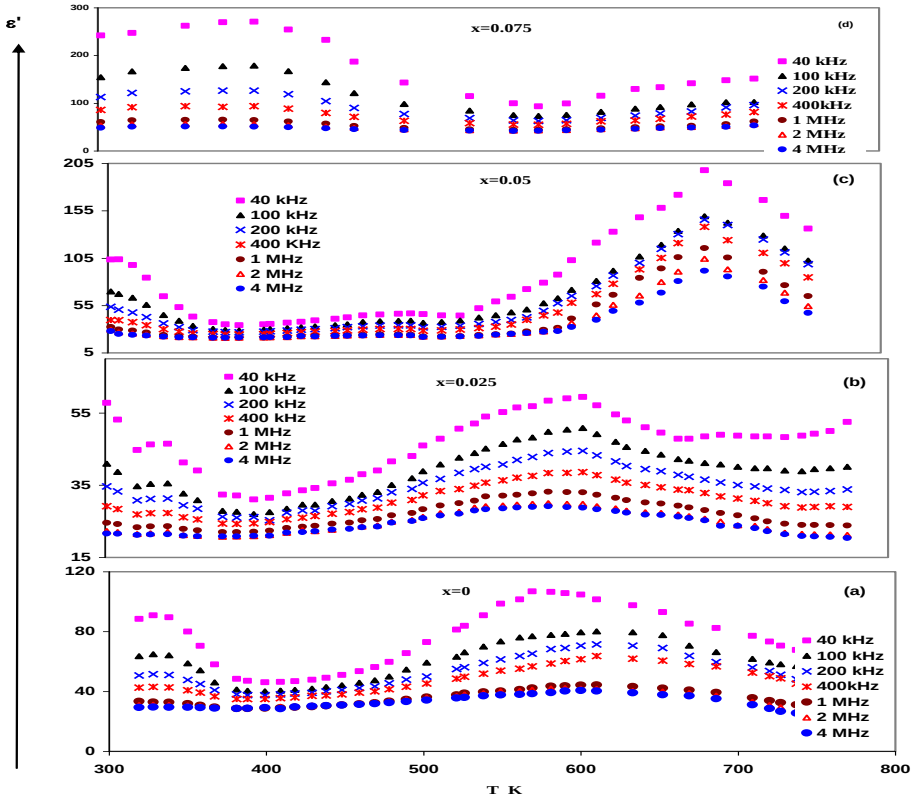

Fig. (7: a- d): The variation of ε ' at different temperature TK as afunction of different frequency for $Li_{0.5-x}Ag_xFe_{2.5}O_4$nanoferrites.

Figure (8) correlating the relation between ln(σ) and the reciprocal temperature at different frequencies. The figures show for all samples, two regions of temperature with different activation energies, indicating different conduction processes. The observed activation energy values at Table 4 depend on Ag concentration (x) which is slightly increased with Ag content. The values of ln (σ) can be interpreted on the basis of the electronic configuration of the different Ag content.

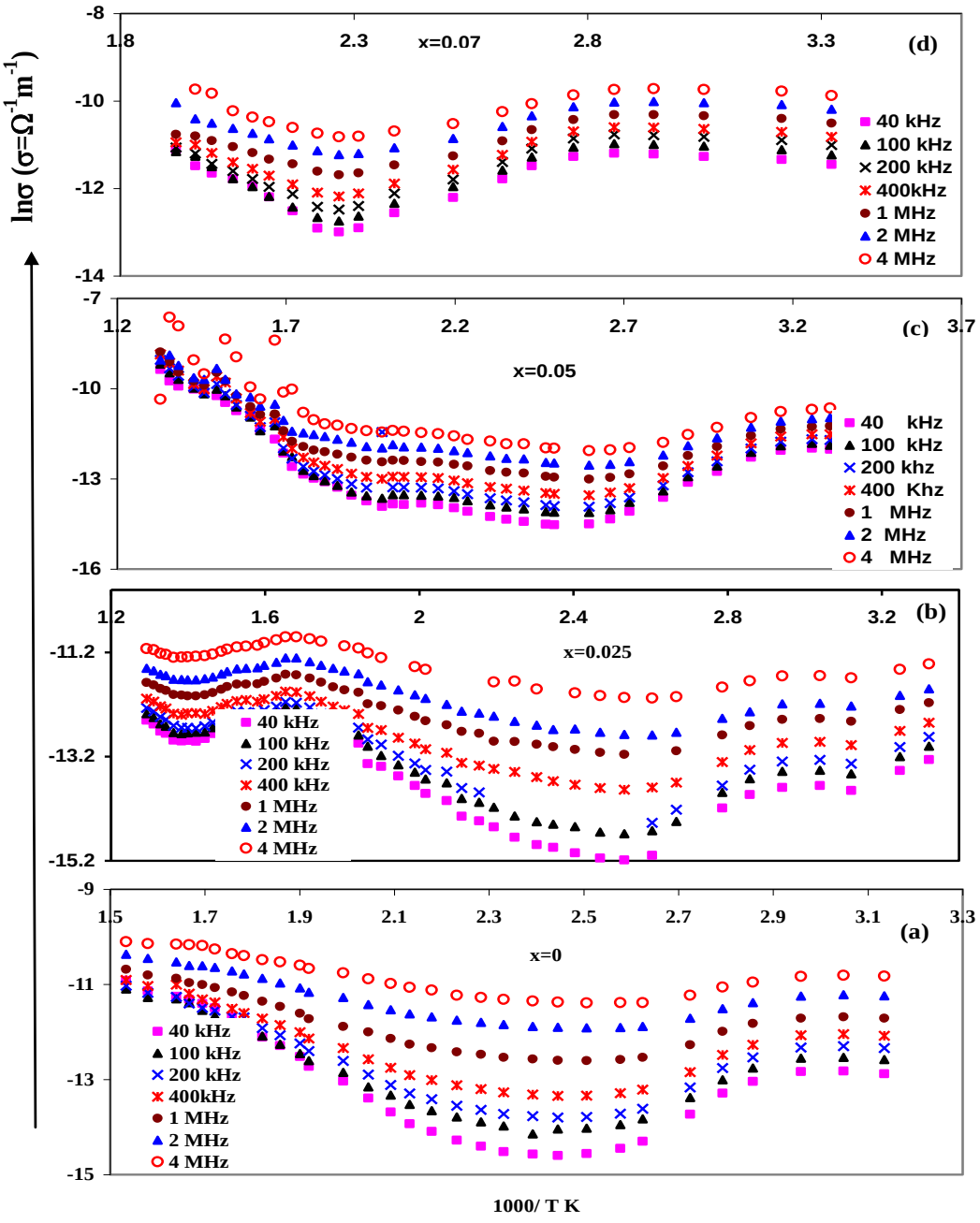

Fig. (8): Variation of ln σ with 1000/TK as a function of frequency.

Table (4): Activation energy in ferrimagnetic; E_1 (eV) and paramagnetic; E_{11} (eV) regions and the transition temperature (T_d) for $Li_{0.5-x}Ag_xFe_{2.5}O_4$; $0.0 \leq x \leq 0.075$ nanoferrites.

T_d (K)	E_{11} (eV)	E_1 (eV)	Ag content(x)	Formula
419	0.12	0.1	0	$Li_{0.5}Fe_{2.5}O_4$
686	0.15	0.12	0.025	$Li_{0.475}Ag_{0.025}Fe_{2.5}O_4$
605	0.16	0.13	0.05	$Li_{0.45}Ag_{0.05}Fe_{2.5}O_4$
569	0.2	0.17	0.075	$Li_{0.425}Ag_{0.075}Fe_{2.5}O_4$

4. Conclusion

1. $Li_{0.5-x}Ag_xFe_{2.5}O_4$; x=0, 0.025, 0.05, 0.075, 0.1 were successfully synthesized using the citrate precursor method without subsequent heat treatment.

2. All the prepared samples exhibit a single phase with cubic spinel structure.

3. The crystallite sizes for silver (Ag) metal cation doped lithium ferrite samples are between 44 to 49 nm is smaller than single domain crystallite size (70 nm), which makes it most suitable for application in high density recording media.

4. The highest value of magnetic susceptibility χ_M = 24. 9 emu/g. mole at Ag content = 0.075 which consider the critical concentration and this value is higher than 1.17 times the undoped sample.

5. The presence of silver ions in the investigated ferrite improves the Curie temperature 1.1 times on the undoped sample.

6. The value of saturation magnetization increase with Ag substitutions and reaches a maximum value of 69 emu/g. mole at x = 0.075 higher than the undoped sample (50 emu/g. mole).

7. The activation energy at x=0.075 is improved 17 times on the undoped sample.

8. The highest value of ε' at x=0.075 can be used for Phase shifter, circulators, microwave component applications.

References

A. N. Shipway, E. Katz, and I.Willner, Chem. Phys. Chem., **1,18(2000**).

A. Dogra, R. Kumar, S.A. Khan, V.V. Siva Kumar,N. Kumar, M. Singh, Nuclear Instruments and Methods in Physics Research **B 225, 283(2004).**

B. I. Lemon, R. M. Crooks, J. Am. Chem. Soc., **122, 12886**(**2000**).

B.D. Cullity, S.R. Stock, elements of X –ray diffraction, third edition, Prentice Hall, New Jersey,**170** (**2001**).

C**.Y. Tsay, K.S. Liu, T.F. Lin**, J. Magn. Magn. Mater. **209,189(2000**)**.**

C. Kluthe, T. Al-Kassab, R. Kirchheim, Materials Science and Engineering **A353, 112**(**2003**).

Cao Guozhong, Nanostuctures and Nanomaterials, ImperialCollege Press,**6pp** (**2003**).

D. Ravinder, A. Chandrashekhar Reddy, Mater. Lett**. 57, 2855 (2003).**

DH. Han, JP. Wang and HL.Lou J. Magn**.** Magn. Mater. **136(1-2),176 (1994).**

E. Hao, H. Sun, Z. Zhou, J. Liu, B. Yang, J. Shen, Chem. Mater., **11, 3096 (1999).**

E. Wolska, K. Stempin, O. Krasnowska-Hobbs, SolidState Ionics **101, 527 (1997).**

FM. Chang, M. Jansen, Krist. Z. **169, 295 (1984).**

G.M. Argentina, P.D. Baba, IEEE Trans. Tech.MTT **22, 652 (1974)**

GM. Kale and T. Asokan, Applied Physics Letters**62(19), 2324 (1993).**

G. Sperka, HP. Fritzer, J. Solid State Commune., **65, 1275 (1988).**

H. Shokrollahi, K. Janghorban, Iranian J. Sci. Technol., Trans. B Eng. **30, 413 (2006).**

H. Shokrollahi, K. Janghorban, J. Magn. Magn. Mater. **308, 238 (2007)**.

I.P. Gilbert, V. Moorthy, S.J. Bull, J.T. Evans, A.G. Jack, J. Magn. Magn. Mater. **242/245, 232 (2002).**

I. Chicinas, O. Geoffroy, J. Magn. Magn. Mater**. 290/291, 1531 (2005).**

I. Soibam, S. Phanjoubam, C Prakash, J. Magn. Magn. Mater. **321, 2779(2009).**

J.R. Dahn, U. Vomsacken, C.A.Micha, SolidState Ionics **44, 87 (1990).**

J. Jiang, Y.M. Yang, L.C. Li, Phys**. B 399, 105 (2007).**

J.R. Hook, H.E. Hall, SolidState Physics, Wiley, New York, (**1991**).

KH. Song, SX. Dou, CC. Sorrell, J. Phys. **C, 185, 2387 (1991).**

K.V. Kumar, D. Ravinder, Int. J. Inorg. Mater. **3, 661 (2001).**

L.A. Dobrazanski, M. Drak, J. Mater. Process. Technol. **157/158, 650 (2004).**

L.A. Dobrzanski, M. Drak, J. Mater. Process. Technol. **175, 149 (2006).**

M.P. Horvath, J. Magn**.** Magn. Mater. **215/216, 171 (2000).**

M. A. Correa-Duarte, M. Giersig, L. M. Liz-Marzan, Chem. Phys. Lett., **286, 497** (**1998**).

M.A. Ahmed, N.O. Kasha, S.I. El-Dek, Nanotechnology **19,0656036 (2008).**

M.N. Obrovac, O. Mao, J.R. Dahn, SolidState Ionics **112, 9 (1998).**

M.T. Buscaglia, V. Buscaglia, M. Viviani, J. Petzelt, M. Savinov, L. Mitoseriu, A. Testino, P. Nanni, C. Harnagea, Z. Zhao, M. Nygren, Nanotechnology **15**, **1113 (2004).**

M.A. Ahmed, S.I. El-dek, S.F. Mansour, N. Okasha, Solid State Sciences **154**, **1 (2010).**

N. Okasha, J. Mater. Sci. **43,4192 (2008**).

R.G. Kharabe, R.S. Devan, C.M. Kaanamadi, B.K. Chougule, Smart Mater.Struct. **15, N36(2006**).

S. Shiojiri, T. Hirai, I.Komasawa, Chem. Commun**., 1439 (1998).**

S. Yamamoto, S. Horie, N. Tanamachi, J. Magn. Magn. Mater. **235, 218 (2001).**

S. Verma, J. Karande, A. Patidar, P.A. Joy, Mater. Lett. **59, 2630 (2005**).

S.J. Manoharan, K.C. Patil, J. Am. Ceram. Soc. **75, 1012 (1992).**

S.S. Bellad, B.K. Chougule, Mater. Chem. Phys. **66, 58 (2000).**

S.H. Hong, J.H.Park, Y.H. Cho, J. Kim, Journal of Magn. and Magn. Mater. **291,1559 (2005).**

V. Verma, S.P. Gairola, V. Pandey, J.S. Tawale, Hua Su, R.K. Kotnala, J. Magn. Magn. Mater. **321, 3808 (2009).**

V.P. Reddy, D.V. Reddy, J. Magn. Magn. Mater. **136, 279 (1994).**

V. Scatturin, P. Bellom, AJ. Salkind , Ric. Sci. **30, 1034 (1960).**

Y. Sakurai, H. Arai, J. Yamaki, Solid State Ionics **113, 29 (1998).**

Yen-Pei Fua, Chin-Shang Hsu, SolidStateCommun. **134, 201 (2005).**

Y.C. Venudhar, K. Satya Mohan, Mater. Lett. **54,135 (2002).**

الملخص باللغة العربية

انتقاء الافضل من الخواص الفيزيائيه لنانو فيريت الليثيوم – الفضة باستخدام طريقه السيتريت

نجوى عكاشة مراد [1]، مها محسن السيد أحمد[2]

1.استاذ الجوامد- قسم الفيزياء- كلية البنات- جامعة عين شمس.

2. معمل علوم المواد (1) – قسم الفيزياء- كلية العلوم- جامعة القاهرة

تم تحضير عينات Li- Ag النانومتريةبطريقة السيترات التى تعتبر من اشهر طرق التحضير الحديثة، وقد تكونت العينات

- حيث تمت بخلط عناصر المركب حسب الاوزان الجزيئية لهذة العناصر مع تغيير نسبة الفضة على حساب الليثيوم من خلال المعادلة $Li_{0.5-x}Ag_xFe_{2.5}O_4$; x = 0.0, 0.025, 0.05, 0.075, 0.1

لتحديد التركيز الحرج من هذة التركيزات المختلفة ،وقد تم فحص العينات بتقنية حيود الاشعة السينية للتاكد من تكوين العينات فى الطور الأحادى، وتحليل الموجات تحت الحمراء لمعرفة التغييرات الكيميائية التى تحدث للمركب اثناء التفاعل والميكروسكوب الالكترونى النافذ لتعيين شكل وحجم الجسيمات المتكون منها المركب، وقد تم دراسة الخواص المغناطيسية لهذه التركيزات بقياس القابلية المغناطيسية وايضا الخواص الكهربية من خلال تعيين ثابت العزل والمقاومة، وقد ظهر ان اعلى قيمة عند تركيز الفضة0.075 وتم قياس التخلف المغناطيسى للعينات السابقة و توافقت النتائج مع القابلية المغناطيسية باعلى قيم لنفس التركيز السابق و اعتبر هو افضل تركيز فى هذا المدى من التركيزات.